

Circulation

JOURNAL OF THE AMERICAN HEART ASSOCIATION



Biglycan Deficiency Causes Spontaneous Aortic Dissection and Rupture in Mice
Anne-Marie Heegaard, Alessandro Corsi, Carl Christian Danielsen, Karina L. Nielsen,
Henrik L. Jorgensen, Mara Riminucci, Marian F. Young and Paolo Bianco
Circulation 2007;115:2731-2738; originally published online May 14, 2007;

DOI: 10.1161/CIRCULATIONAHA.106.653980

Circulation is published by the American Heart Association, 7272 Greenville Avenue, Dallas, TX 75214

Copyright © 2007 American Heart Association. All rights reserved. Print ISSN: 0009-7322. Online ISSN: 1524-4539

The online version of this article, along with updated information and services, is located on the World Wide Web at:

<http://circ.ahajournals.org/cgi/content/full/115/21/2731>

Subscriptions: Information about subscribing to *Circulation* is online at
<http://circ.ahajournals.org/subscriptions/>

Permissions: Permissions & Rights Desk, Lippincott Williams & Wilkins, a division of Wolters Kluwer Health, 351 West Camden Street, Baltimore, MD 21202-2436. Phone: 410-528-4050. Fax: 410-528-8550. E-mail:
journalpermissions@lww.com

Reprints: Information about reprints can be found online at
<http://www.lww.com/reprints>

Biglycan Deficiency Causes Spontaneous Aortic Dissection and Rupture in Mice

Anne-Marie Heegaard, MD, PhD*; Alessandro Corsi, MD, PhD*; Carl Christian Danielsen, MD; Karina L. Nielsen, PhD; Henrik L. Jorgensen, MD, PhD; Mara Riminucci, MD, PhD; Marian F. Young, PhD; Paolo Bianco, MD

Background—For the majority of cases, the cause of spontaneous aortic dissection and rupture is unknown. An inherited risk is associated with Marfan syndrome, Ehlers-Danlos syndrome type IV, and loci mapped to diverse autosomal chromosomes. Analysis of pedigrees however has indicated that it may be also inherited as an X-linked trait. The biglycan gene, found on chromosome X in humans and mice, encodes a small leucine-rich proteoglycan involved in the integrity of the extracellular matrix. A vascular phenotype has never been described in mice deficient in the gene for small leucine-rich proteoglycans. In the breeding of BALB/cA mice homozygous for a null mutation of the biglycan gene, we observed that 50% of biglycan-deficient male mice died suddenly within the first 3 months of life.

Methods and Results—Necropsies revealed a major hemorrhage in the thoracic or abdominal cavity, and histology showed aortic rupture that involved an intimal and medial tear as well as dissection between the media and adventitia. By transmission electron microscopy and biomechanical testing, the aortas of biglycan-deficient mice showed structural abnormalities of collagen fibrils and reduced tensile strength. Similar collagen fibril changes were observed in male as well as in female biglycan-deficient mice, which implies a role of additional determinants such as gender-related response to stress in the development of this vascular catastrophe only in male mice.

Conclusions—The spontaneous death of biglycan-deficient male mice from aortic rupture implicates biglycan as essential for the structural and functional integrity of the aortic wall and suggests a potential role of biglycan gene defects in the pathogenesis of aortic dissection and rupture in humans. (*Circulation*. 2007;115:2731-2738.)

Key Words: aneurysm ■ biglycan ■ gene targeting

The biglycan (*BGN*) gene, found on chromosome X in humans and mice,¹ encodes a member of the expanding family of small leucine-rich proteoglycans (SLRPs). Their core protein is composed of tandem-linked repeats of ≈25 amino acid long, leucine-rich motifs to which glycosaminoglycan chains are attached. BGN contains 10 leucine-rich repeats, and its 40-kDa core protein binds 2 chondroitin- or dermatan-sulfate glycosaminoglycan chains.² In agreement with the high expression of BGN in bone,³ *bgn*-deficient mice have been reported to show a phenotype characterized by growth failure, reduced bone formation, and age-related severe osteopenia.⁴ This phenotype however has been described to be fully expressed in male but not in female mice.⁵ Recently, dental and muscular abnormalities, thinning of the skin, and osteoarthritis have been also described in these mice

(for review see Young et al⁶). The demonstration of tissue-specific abnormalities of collagen fibrils in different collagenous matrices, such as bone, dermis, and tendon,^{7–8} indicates that BGN plays a critical role in the control of collagen fibrillogenesis and in the proper assembly of the extracellular matrix.

Editorial p 2687 Clinical Perspective p 2738

Normal arteries are sites of expression and deposition of SLRPs, in particular decorin and BGN.^{3,9,10} Abnormalities in their expression or deposition have been described in diverse human vascular disease, such as aneurysm and dissection.^{11–14} For the majority of cases, the cause of aortic dissection in humans is unknown. Marfan syndrome and

Received July 24, 2006; accepted March 13, 2007.

From the Department of Pharmacology and Pharmacotherapy (A.H.), Faculty of Pharmaceutical Sciences, University of Copenhagen, Copenhagen, Denmark; Nordic Bioscience A/S (A.H., K.L.N.), Herlev, Denmark; Department of Experimental Medicine and Pathology (A.C., P.B.), Università La Sapienza, Rome, Italy; Department of Connective Tissue Biology (C.C.D.), Institute of Anatomy, University of Aarhus, Aarhus, Denmark; Department of Clinical Biochemistry (H.L.J.), Bispebjerg University Hospital, Copenhagen, Denmark; Department of Experimental Medicine (M.R.), Università dell'Aquila, L'Aquila, Italy; Parco Scientifico Biomedico San Raffaele (M.R., P.B.), Rome, Italy; Craniofacial and Skeletal Diseases Branch (M.F.Y.), National Institute of Dental and Craniofacial Research, National Institutes of Health, Bethesda, Maryland.

*The first 2 authors contributed equally to this work.

Correspondence to Dr Anne-Marie Heegaard, Department of Pharmacology and Pharmacotherapy, The Danish University of Pharmaceutical Sciences, Universitetsparken 2, DK-2100 Copenhagen, Denmark (e-mail amhe@farma.ku.dk) or Dr Paolo Bianco, Department of Experimental Medicine and Pathology, Section of Pathology, University La Sapienza, Viale Regina Elena 324, 00161 Rome, Italy (e-mail p.bianco@flashnet.it).

© 2007 American Heart Association, Inc.

Circulation is available at <http://www.circulationaha.org>

DOI: 10.1161/CIRCULATIONAHA.106.653980

Ehlers-Danlos syndrome (EDS) type IV, and a few other, more rare, genetic disorders are associated with an inherited risk of aortic dissection.^{15–16} Nonsyndromic familial susceptibility to aortic dissection and rupture has also been established,^{17–22} and analysis of pedigrees has indicated that the risk for aortic dissection may be inherited as a X-linked trait.²³ Interestingly, even though primary genetic defects in the *BGN* encoding gene have not been reported in humans, *BGN* mRNA and protein expression levels are altered in patients with Turner syndrome¹ and vascular anomalies, such as aortic dissection and rupture, are frequently observed in these patients.²⁴

A vascular phenotype has never been described in *SLRPs*-deficient mice, which include the original *bgn*-deficient (*bgn*-knockout (KO)) 129Sv/C57BL6 mice.⁴ In the breeding of BALB/cA mice homozygous for a null mutation of the *BGN* encoding gene, we observed that male *bgn*-KO mice died suddenly before 2 to 3 months of age. To investigate the vascular phenotype of these mice we have conducted a histological, ultrastructural, and biomechanical analysis of the aortas of biglycan-deficient and wild-type (WT) mice.

Methods

Mice

bgn-KO mice with a 129Sv/C57BL6 background⁴ were backcrossed into a BALB/cABomTac (Taconic M&B A/S, Ry, Denmark) background for at least 7 generations. More than 300 offspring mice from backcross and intercross breeding were genotyped and observed for sudden death. The distribution of genotypes was as follows: 69 *bgn*^{+/+}; 56 *bgn*^{+/-}; 15 *bgn*^{-/-}; 65 *bgn*⁺⁰; 74 *bgn*⁻⁰; 54 were not determined. The lower number of *bgn*^{-/-} mice was the result of the breeding setup. During a period of 5 months, 22 mice were autopsied and further analyzed by histology. The mice were all housed together, and all litters were affected. Age-matched mice with the BALB/cA background derived from crossing heterozygous (*bgn*^{+/-}) female mice with either WT (*bgn*⁺⁰) or *bgn*-KO (*bgn*⁻⁰) male mice were used for ex vivo studies. Four *bgn*-KO male, 4 WT male, 3 *bgn*-KO female, and 2 WT female mice (age 2.5 to 3 months) were used for transmission electron microscopy analysis, and 13 four-month-old and 16 ten-month-old male mice were used for the strength measurements. All mice were euthanized. Animals were housed under standard conditions (free access to a standard mouse diet and water, 12-hour light/dark cycle) as approved by the Experimental Animal Committee, The Danish Ministry of Justice. Genotypes were determined by a polymerase chain reaction–based assay as previously described.⁵

Tissue and Histology

Aortas with heart, lungs, and kidneys were isolated within 30 minutes of death from male *bgn*-KO mice that died spontaneously, and from 3 months old male and female *bgn*-KO and WT mice. The samples were fixed in 4% formaldehyde (freshly made from paraformaldehyde) in phosphate buffer (0.1 mol/L, pH 7.2), cross-sectioned, and routinely processed for paraffin embedding. Sections (5 μ m thick) were stained with hematoxylin-eosin and Alcian blue (pH 2.5) for acid proteoglycans, Mallory's trichrome for collagen fibers, and Weigert for elastic fibers.²⁵

Immunohistology

Immunolocalization of BGN was performed as described previously⁴ by means of an indirect immunoperoxidase protocol with a polyclonal antiserum to mouse BGN core protein (LF106).²⁶ The LF106 antiserum was used at a dilution 1:100 in PBS–0.1% BSA for 2 hours at room temperature. Because the LF106 antiserum recognizes protein cores devoid of attached glycosaminoglycans chains, sec-

tions were treated with 1.25 U/mL chondroitin ABC lyase (protease-free, from *Proteus vulgaris*; ICN, Covina, Calif.) as described previously.³

Transmission Electron Microscopy

Fixed samples were washed overnight in cacodylate buffer at 4°C. After post-fixation for 1 hour at 4°C with 1% osmium tetroxide in cacodylate buffer, samples were treated with tannic acid as en bloc stain to enhance the contrast of elastic laminae as described previously.²⁷ Samples were rinsed in water, dehydrated in a graded series of ethanol to propylene oxide and infiltrated and embedded in epoxy resin (Agar Scientific Ltd, Stansted, Essex, UK). Semithin sections were stained with Azur II-methylene blue and examined with a light microscope to select appropriate fields. Ultrathin sections were contrasted with uranyl acetate and lead citrate and examined with a CM Philips transmission electron microscope (KE Electronics, Tofts, UK). For quantitative studies, collagen fibril diameter and density were measured on photographic prints as described previously.²⁸ Mean density values were calculated from 3 to 5 μ m² per mouse from 4 *bgn*-KO males; 3 WT males; 3 *bgn*-KO females and 2 WT females before group means (\pm SD) was calculated. For diameter of collagen fibril profiles, measurements were obtained from a total of 3083 collagen fibril profiles (*bgn*-KO male, *n*=769; WT male, *n*=707; *bgn*-KO female, *n*=799; WT female, *n*=808) counted in 4 μ m² of each group (2 animals per group) as described previously.²⁹

Immuno-Electron Microscopy

The technique was performed with an immunogold protocol as described previously.³⁰ LF106 and polyclonal anti-type III collagen (Santa Cruz Biotechnology, Inc., Santa Cruz, Calif.) were used at a 1:10 dilution in PBS–0.1% BSA. Ultrathin sections to be incubated with LF106 were pretreated with 1.25 U/mL chondroitin ABC lyase in 0.1 mol/L Tris, 0.05 mol/L calcium acetate, 0.01% BSA (pH 7.2) for 5 minutes at 37°C. After incubation with undiluted normal goat (Sigma, St. Louis, Mo.) or rabbit (Dako, Glostrup, Denmark) serum, ultrathin sections were incubated with LF106 or anti-type III collagen for 1 hour, and after repeated washes with PBS, with gold-labeled (particle size 10 nm) goat anti-rabbit (BioCell, Cardiff, UK) or rabbit anti-goat (Sigma) immunoglobulins, respectively, both diluted 1:20 in PBS–0.1% BSA for 30 minutes. Incubations were performed at room temperature. Control sections were labeled with a primary antibody of unrelated specificity or normal serum. Sections stained for type III collagen were used to estimate the density of gold particles on the collagen fibrils of the adventitia (number per μ m²) as previously described.³¹

Biomechanical Testing

Aortas were isolated from age-matched male *bgn*-KO and WT mice that were euthanized at 4 months and 10 months of age. Sampled aortas (6 to 9 per group of mice) were stored at –20°C until analysis in 50 mmol/L Tris/HCl (pH 7.4). The buffer was used throughout the testing procedure. Before testing, lower thoracic and upper abdominal aorta was cleaned of adhering fat and loose connective tissue. Aortic rings (1-mm high, 2 to 5 specimens per mouse, in average 4.4 specimens per mouse in the 4-month-old WT group, 4.1 specimens per mouse in the 4-month-old *bgn*-KO group, and 3 specimens per mouse in both 10-month-old groups) were cut between intercostal arteries and abdominal arterial branches. The ring height was measured in a microscope equipped with a calibrated ocular micrometer, and the mean radial thickness of the aortic wall was measured by an electronic length gauge (Heidenhain, Traunreut, Germany) on wet specimens flattened between 2 parallel surfaces under a fixed load. Specimens were mounted in a material testing machine (Alwetron TCT5, Lorentzen & Wettre, Stockholm, Sweden) with 2 parallel steel wires (diameter 0.35 mm) through the lumen, and then radially stretched (10 mm/min) until failure while soaked in buffer at room temperature. After failure, the collagen content in the ring specimens was measured by hydroxyproline determination as previously described.³² Maximum load and stiffness were calculated. The

values were divided by 2 to represent a single width of the aortic wall. The original circumference of the ring specimen was defined as the circumference at which the specimen attained a minimal load (1% of maximum). Mean values of the mechanical parameters as well as the aortic diameter, wall thickness, and collagen content were obtained for each mouse before group means (\pm SD) were calculated.

Statistical Analysis

Results for density of gold particles and diameter of collagen fibril profiles are presented as median and percentiles (25% and 75%) and those for density of collagen fibril profiles, mechanical parameters, aortic diameter, wall thickness, and collagen content as means (\pm SD). The difference in the density of gold particles between male *bgn*-KO and WT was analyzed by Student *t* test for unpaired data. Linear mixed-model analysis (PROC MIXED, SAS, Cary, N.C.) was used to test the effect of *bgn*-KO and gender on collagen fibril density and diameter with a random effect for animal. Two-way ANOVA was used to test the effect of *bgn*-KO and age on mechanical parameters, aortic diameter, wall thickness, and collagen content. Log transformation was performed as appropriate to obtain normality and variance homogeneity. A probability level of 5% was used to establish significance of differences.

The authors had full access to and take full responsibility for the integrity of the data. All authors have read and agreed to the manuscript as written.

Results

Vascular Phenotype in Male *bgn*-KO Mice

About 50% of the male *bgn*-KO mice but neither the *bgn*-KO female nor the wild-type (WT) mice suddenly died before 2 to 3 months of age (average lifespan 9.3 ± 0.3 weeks). One of the mice died while its ear was punched, and another died after placement with females for breeding. Necropsies performed on 22 *bgn*-KO male mice revealed that the mice died from a massive hemorrhage in the thoracic (82%) or abdominal cavity (18%) (Figure 1a). Histological studies (Figure 1b to 1h) showed aortic rupture with the rupture across the intima and the media and dissection of the aortic wall with blood collection between media and adventitia. Fragmentation of elastic layers, deposits of myxoid matrix, and dissection within the aortic media, which represent the hallmarks of Marfan-like dissection,^{33–34} were not observed in *bgn*-KO mice.

Because the pattern of aortic dissection observed in male *bgn*-KO with blood collection between media and adventitia represented a phenocopy of that observed in *col3a1*-KO mice,²⁹ and depletion of a single noncollagenous protein in the extracellular matrix may profoundly alter the overall matrix stoichiometry, we asked whether a common molecular basis could underlie the aortic dissection and rupture in *bgn*- and *col3a1*-KO mice. Specifically, we asked if a secondary reduction in type III collagen could be brought about by *BGN* deficiency. Quantitative transmission electron microscopy immunolocalization of type III collagen, however, revealed no difference in amount of labeling (Figure 1i) in the aortas of *bgn*-KO mice compared with WT mice.

Biglycan Immunolocalization in the Normal Mouse Aorta

To further investigate the link between the specific pattern of aortic rupture observed in *bgn*-KO mice and *BGN*-deficiency itself, the pattern of BGN localization in the aortas of WT mice was determined. Immunohistochemistry demonstrated

that of the 3 layers of the aortic wall, the adventitia is in fact the major site of BGN deposition in the mouse. Prominent immunostaining of the adventitia and only minimal labeling in the media and intima were detected at the light microscopy level (Figure 2a and 2b). Transmission electron microscopy immunolocalization further demonstrated that most of BGN-immunoreactive sites in the aorta were associated with collagen fibrils (Figure 2c and 2d), which are much more numerous and densely spaced in the adventitia compared with the media. However, in keeping with previous studies that report the presence of BGN within elastin fibers,³⁵ additional sites of *BGN* immunoreactivity were detected within the elastin-associated electron dense (microfibril) phase, which accounts for a minor proportion of the elastic fiber mass (Figure 2e and 2f). These findings predicted that the most prominent structural changes would be expected to occur in the adventitia as a result of *BGN* deficiency.

Structural Defects in the Aortas of *bgn*-KO Mice

Comparative light microscopy analysis of the aortas of male *bgn*-KO and WT mice failed to reveal abnormalities in the overall organization of the tunica media and adventitia (Figure 3a to 3d). In contrast, comparative transmission electron microscopy analysis revealed distinct abnormalities of collagen fibrils in the aortas of *bgn* KO mice (Figure 3e to 3h), including marked variations in size and shape, and ragged or notched cross-sectional profiles. These changes resemble those previously observed in dermis, bone and tendon of *bgn* KO mice^{7–8} and were highly reminiscent of those occurring in diverse human EDSs.^{36–37} Despite these collagen fibril changes, aortic diameter, wall thickness, and collagen content in the aortic ring specimens from 4- and 10-month-old male *bgn*-KO and WT mice (Table) were not different ($P > 0.14$).

Biomechanical Properties of the Aortas of *bgn*-KO Mice

Because collagen fibrils were found to be abnormal and collagen is the main determinant of vessel tensile strength, the resistance to radial elongation of aortic ring specimens from male *bgn*-KO and WT mice was compared. Mechanical testing of aortic rings subjected to radial elongation revealed that load-strain curves for *bgn*-KO and WT mice essentially coincided during initial (elastic) deformation (Figure 4a). This reflected the integrity of all arterial wall coats and the contribution of an intact media to overall energy absorption and deformation. However, the maximum load withstood by KO specimens (Figure 4b) and their maximum stiffness (Figure 4c) were significantly lower (50% to 70%) compared with WT. Energy absorption until failure was also reduced to a similar extent (47% to 58%) in the KO specimens compared with WT (2-way ANOVA: *bgn*-KO $P < 0.0001$; age $P > 0.45$). Importantly, the vessel wall failed in a stepwise fashion, and failure at maximum load corresponded to the rupture of the medial coat alone, as observed by video recording during testing at a magnification of about $\times 40$, and confirmed by amido black surface staining of the arterial coats (data not shown). After the failure of the media, the adventitia sustained further strain before failing in 1 or more steps. The

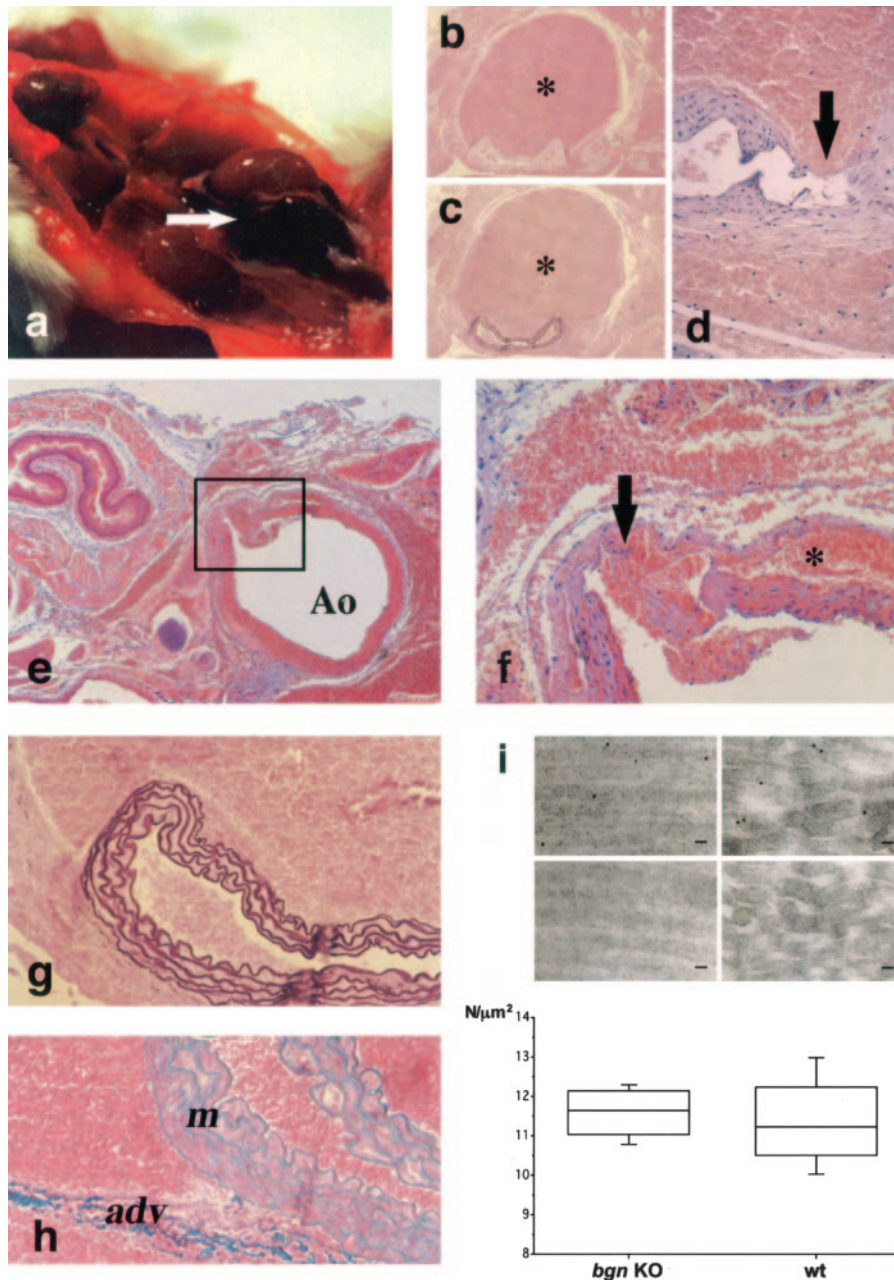


Figure 1. Vascular phenotype in male *bgn*-KO mice. a, Male *bgn*-KO mouse with a blood clot (arrow) on the posteromedial surface of the left kidney. b through f, Dissection of the abdominal and thoracic aorta are illustrated in b to d and e to f, respectively. The intima and media are ruptured (arrow in d and f) and blood-filled thoracic aorta and adventitia (* in b, c, and e to f). Detail of the boxed area in e. Stains for elastin (g) and collagen (h) fibers showed integrity of the elastic laminae of the tunica media (g) and the separation of the media from the adventitia (h). i, Quantitative electron microscopy immunolocalization of type III collagen (upper panels: staining for type III collagen; bottom panels: negative controls), calculated as density of gold particles (per μm^2) within the adventitia, failed to reveal significant difference between male *bgn*-KO and age- and gender-matched WT mice. Staining in b, d, e, and f: hematoxylin-eosin; staining in c and g: Weigert for elastic fibers; staining in h: Mallory for collagen fibers. Bar in i is 50 nm. Ao indicates aorta; adv, adventitia; and m, media.

height of the load-strain curve for strain values after medial failure thus reflected solely the mechanical strength of the collagenous adventitia. Interestingly, as shown in Figure 4a, the difference in load sustained by the adventitia was closely similar to the difference in maximum load sustained by the entire aortic ring at failure of the media, which indicated that the reduced performance of the adventitia explains most of the observed reduced strength of KO aortic specimens.

Gender Effect of *BGN* Deficiency

Because death caused by aortic rupture was apparently male-specific in *bgn*-KO mice, we asked whether the observed changes in collagen fibril structure were in turn male-specific. Both male and female *bgn*-KO mice demonstrated similar changes in fibril shape and range (Figure 5a) when compared with WT mice. The collagen fibrils were counted and mean density (per μm^2) were calculated for each

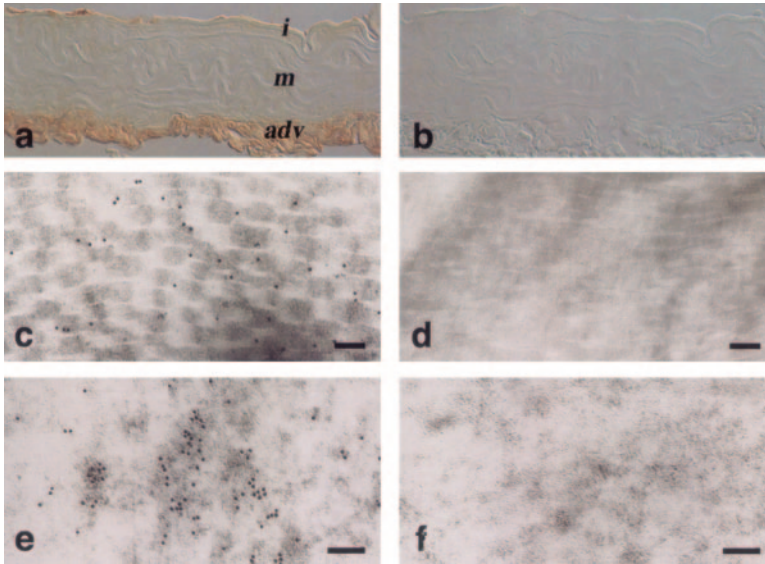


Figure 2. Biglycan immunolocalization in the aortas of WT mice. By light microscopy, biglycan core protein is mainly localized within the adventitia (*adv*). Faint staining was also observed within the intima (*i*) and the media (*m*) (*a*). By means of immuno-electron microscopy, biglycan core protein localizes on collagen fibrils of the adventitia (*c*) and within the elastin-associated electron-dense (microfibril) phase of the tunica media (*e*). Negative controls are illustrated in *b*, *d*, and *f*. Bar in *c* to *f* is 100 nm.

group (mean \pm SD; male *bgn*-KO: 187.4 \pm 6.9; male WT: 177.8 \pm 1.5; female *bgn*-KO: 191.3 \pm 8.4; female WT: 192.5 \pm 2.1). Linear mixed-model analysis revealed no significant differences between genotypes. However, significant difference in mean density was found between WT male and female mice ($P=0.01$). In contrast, when the collagen fibril diameter was analyzed with a linear mixed-model, significant differences were found between both genotypes and genders ($P<0.0001$). The collagen fibril diameter was significantly lower in *bgn*-KO males compared with WT males and *bgn*-KO females (Figure 5b). Interestingly, the collagen fibril diameter was also significantly lower in WT males compared with WT females, consistent with previous indications of a gender related difference in collagen fibril diameter in mice independent of the *bgn*-KO genotype.³⁸

Discussion

Either alone or when combined with deficiencies in other SLRPs, BGN deficiency in mice has been associated with skeletal, dental, muscular, and skin abnormalities, as well as with osteoarthritis and ectopic tendon ossification.^{4,6–8} Collagen fibril changes^{7,8} that are highly reminiscent of those observed in different tissues of diverse EDSs^{36,37} underlie the different tissue-specific phenotypes observed in *bgn*-KO mice. In the present article, we document that similar changes

occur in the collagen fibrils of the aortic wall, which lead to reduced tensile strength and spontaneous dissection and rupture.

The pattern of aortic dissection observed in male *bgn*-KO mice is different from that commonly observed in Marfan-like human aortic dissection and similar to that observed in *col3a1*-deficient mice,²⁹ the mouse model of human EDS-IV. In *bgn*-KO mice and in *col3a1*-deficient mice, dissection of the aortic wall occur between the media and the adventitia rather than within the media, which suggests that a secondary reduction in type III collagen could be brought about by BGN deficiency. However, no differences in the amount of labeling were detected in the aortas of *bgn*-KO mice compared with WT mice, which dispels a secondary change in type III collagen deposition and indicates a direct role of BGN in structural integrity and mechanical performance of the aortic wall.

To better clarify the link between the specific pattern of aortic dissection and rupture observed in *bgn*-KO mice and BGN deficiency itself, we have determined the pattern of BGN distribution in the aortas of WT mice. The demonstration that BGN deposition was mostly associated with collagen fibrils predicted that the most prominent structural and functional changes that resulted from BGN deficiency would be expected to occur in the aortic adventitia, the tunica in

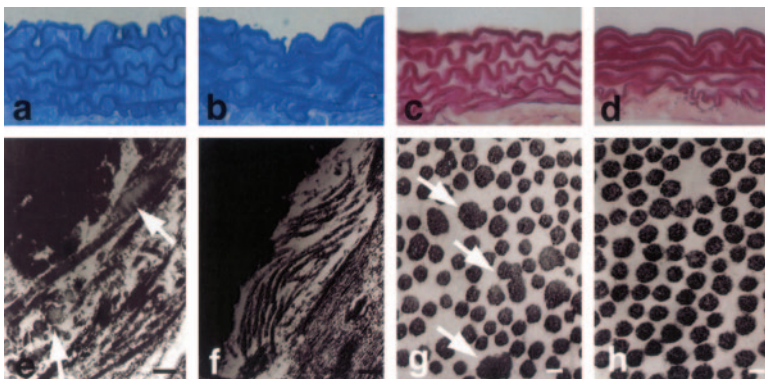


Figure 3. Comparative morphology of the aortas of male *bgn*-KO and WT mice. No morphological differences in the overall organization of the aortic wall are evident by light microscopy (*a* to *d*) between male *bgn*-KO (*a*, *c*) and WT (*b*, *d*) mice. However, compared with WT (*f*, *h*), in the absence of biglycan the collagen fibrils show irregular profiles and greater size variability both in the media (arrows in *e*) and in the adventitia (arrows in *g*). Staining in *a* and *b*: Azur II-methylene blue; staining in *c* and *d*: Weigert's stain for elastic fibers. Bar in *e* and *f* is 100 nm; bar in *g* and *h* is 50 nm.

Mean (\pm SD) Diameter, Wall Thickness, and Collagen Content in 1-mm Aortic Rings From 4- and 10-Month-Old Male *bgn*-KO and WT Mice

	4 Months		10 Months	
	<i>bgn</i> -KO (n=6)	WT (n=7)	<i>bgn</i> -KO (n=7)	WT (n=9)
Diameter, mm*	1.13 \pm 0.09	1.10 \pm 0.06	1.14 \pm 0.04	1.09 \pm 0.05
Wall thickness, μ m*	25.20 \pm 1.50	27.60 \pm 1.80	29.90 \pm 4.10	25.60 \pm 5.00
Collagen content, μ g/mm*	6.00 \pm 1.80	5.60 \pm 0.90	6.30 \pm 1.70	5.50 \pm 0.50

*Two-way ANOVA showed no effect of either *bgn*-KO ($0.15 < P < 0.42$) or age ($0.17 < P < 0.95$) on any of the parameters but showed an unaccountable *bgn*-KO/age interaction in wall thickness ($P < 0.05$).

which collagen fibrils are more abundant to sustain the bulk of hemodynamic stress. As previously observed in other collagenous extracellular matrices in the *bgn*-KO mice,^{7,8} ultrastructural analysis revealed marked variability in size and shape of aortic collagen fibrils. These changes were mirrored by the reduced tensile strength of the aorta, as demonstrated by the significantly lower maximum load and maximum stiffness withstood by KO aortic ring specimens compared with WT specimens. Interestingly, even though BGN deposition was also detected within the media and in particular within the elastin-associated electron-dense (microfibril) phase,³⁵ structural changes in the elastic component of the aorta were not apparent in *bgn*-KO mice. This is in contrast to some mouse models of aortic aneurysm. For instance, targeted deletion of lysyl oxidase, an essential biosynthetic enzyme for collagen and elastin fibers, results in hazy and unruffled elastic lamellae by light microscopy.³⁹ The ability of BGN to form complexes with microfibril-associated glycoprotein 1 and tropoelastin (the soluble precursor of mature elastin) suggests that BGN may be involved in the deposition of tropoelastin onto the surface of the microfibrils during elastinogenesis or, alternatively, in the stabilization of the mature elastic fibers.⁴⁰ However, because tropoelastin can bind fibrillin-1 and -2,⁴¹ the main components of microfibrils, elastinogenesis and elastic fiber stabilization may also occur independently of BGN. In addition, the well established redundant functions of SLRPs^{6,8,42} sug-

gest that other members of the SLRP family, (in particular decorin, given its ability to bind tropoelastin, fibrillin-1, and microfibril-associated glycoprotein 1^{40,43}), may be able to substitute for BGN in both of these processes and further contribute to the explanation of the absence of structural changes in the aortic elastic lamellae of *bgn*-KO mice.

It is of interest that death for aortic rupture was male-specific in *bgn*-KO mice. A gender difference was also observed in the skeletal phenotype, which occurs in male but not in female *bgn*-KO mice.^{4,5} To explain the occurrence of aortic rupture only in male mice, we asked if the changes in collagen fibrils were in turn male-specific. Ultrastructural analysis of the aortas of male and female *bgn*-KO mice revealed the occurrence of comparable abnormalities of collagen fibrils in both genders. The fibril mean diameter, however, was significantly lower in male *bgn*-KO mice compared with either KO female or WT male and female mice. Interestingly, the mean diameter was also significantly lower in male than in female WT mice. Even though a gender-related effect on collagen fibril diameter is well established in mice,³⁸ an additive effect of *BGN* deficiency with respect to a native gender-related difference in fibril structure may be invoked to explain the male-specific nature of aortic dissection and rupture in *bgn*-KO mice. However, this finding does not exclude a contributory role of additional and/or synergic determinants. Gender differences influence the incidence of many diseases and in general they have been

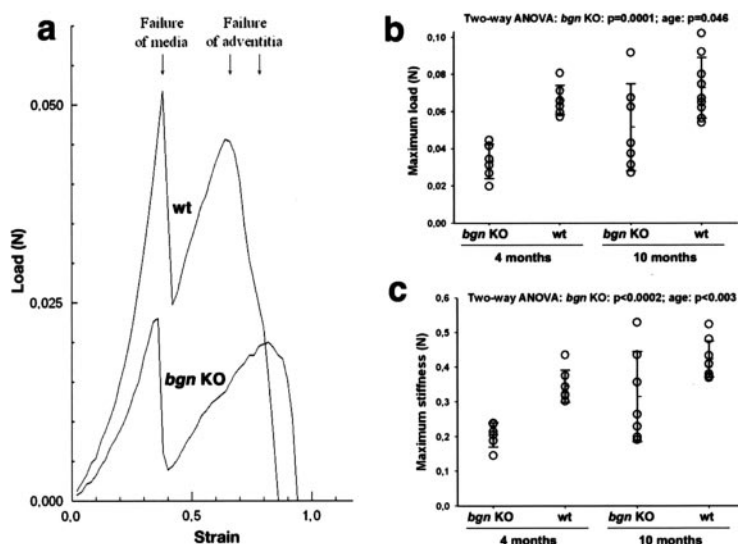


Figure 4. Comparative biomechanical properties of the aortas of male *bgn*-KO and WT mice. a, Representative load-strain curves for aortic rings from 1 *bgn*-KO mouse and 1 age-matched WT mouse are illustrated. The maximum load withstood by KO aortic specimens (b) and their maximum stiffness (c) (mean \pm SD) were significantly lower compared with WT. Both maximum load and maximum stiffness increased with age of mice. Effects of *bgn*-KO and age were tested by 2-way ANOVA; *n* for each group as in the Table.

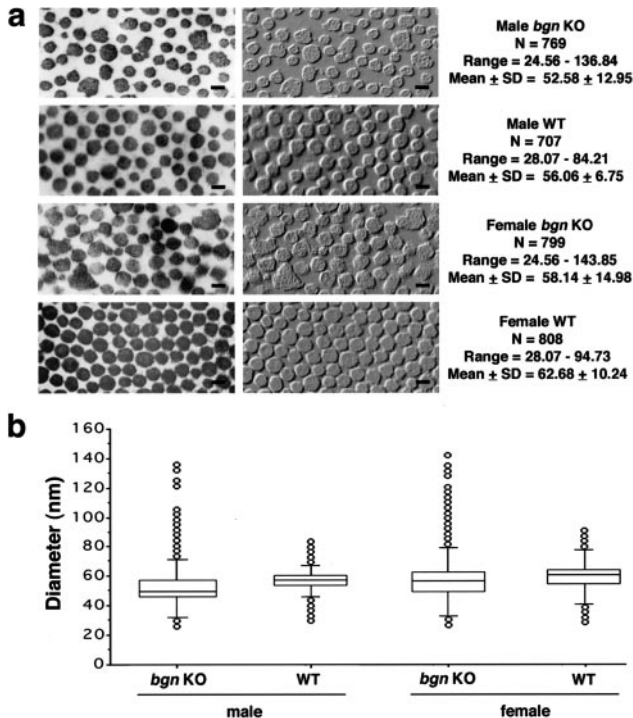


Figure 5. Gender effect of biglycan deficiency on collagen fibrils in male and female *bgn*-KO and WT mice. Morphological comparison of collagen fibril profiles in the aortic adventitia of *bgn*-KO and WT male and female mice. Shape and size variability of collagen fibril profiles are common to male and female gender. The panels on the right are the same images as shown in the panels on the left but were modified with Adobe Photoshop 9.0 to better visualize collagen fibril profiles. The bar is 50 nm. The total number of collagen fibril profiles measured in the different groups was similar and the range of their diameter was increased in both male and female *bgn*-KO compared with their gender-matched WT mice. **b**, Median and percentiles (25% and 75%) of the collagen fibril diameter measured in each group. Linear mixed-model analysis revealed that collagen fibril diameter was significantly lower in *bgn*-KO male compared with WT male ($P < 0.0001$) and *bgn*-KO female ($P < 0.0001$) mice and in WT male compared with WT female ($P < 0.0001$).

interpreted primarily to reflect either estrogen-mediated protection or androgen-mediated susceptibility against pathological conditions.^{44–47} The evidence that 2 male mice died while either its ear was punched or after placement with females for breeding suggest a pathogenetic role of the diverse gender-related estrogen-dependent response to stress.^{44,46}

In humans, abnormalities in *BGN* expression or deposition have been described in diverse vascular diseases such as aortic aneurysm and dissection.^{10–14} For example, *BGN* mRNA and protein have been demonstrated to be reduced in aortas with aneurysms compared with normal aortas.¹⁴ However, a direct causative link between *BGN* deficiency and ruptured aneurysm of the aorta has never been shown, and the cause of spontaneous aortic dissection and rupture remains unknown for the majority of cases. A X-linked mode of inheritance has been identified in some families,²³ and a very high incidence of aortic dissection and rupture is observed in patients with Turner syndrome.²⁴ Taken together, all these findings support our data on *bgn*-KO mice, which points to

BGN as a candidate gene for non-Marfan, non-EDS IV-related risk of aortic dissection and rupture in humans.

Acknowledgments

The authors thank N.T. Foged for his support.

Sources of Funding

This work was supported in part by grants from the Ministry for University and Research of Italy (Dr Bianco).

Disclosures

None.

References

- Geerkens C, Vetter U, Just W, Fedarko NS, Fisher LW, Young MF, Termine JD, Robey PG, Wöhrle D, Vogel W. The X-chromosomal human biglycan gene *BGN* is subject to X inactivation but is transcribed like an X-Y homologous gene. *Hum Genet.* 1995;96:44–52.
- Iozzo RV. The biology of the small leucine-rich proteoglycans: functional network of interactive proteins. *J Biol Chem.* 1999;274:18843–18846.
- Bianco P, Fisher LW, Young MF, Termine JD, Robey PG. Expression and localization of the two small proteoglycans biglycan and decorin in developing human skeletal and non-skeletal tissues. *J Histochem Cytochem.* 1990;38:1549–1563.
- Xu T, Bianco P, Fisher LW, Longenecker G, Smith E, Goldstein S, Bonadio J, Boskey A, Heegaard AM, Sommer B, Satomura K, Dominguez P, Zhao C, Kulkarni AB, Robey PG, Young MF. Targeted disruption of the biglycan gene leads to an osteoporosis-like phenotype in mice. *Nat Genet.* 1998;20:78–82.
- Nielsen KL, Allen MR, Bloomfield SA, Andersen TL, Chen XD, Poulsen HS, Young MF, Heegaard AM. Biglycan deficiency interferes with ovariectomy-induced bone loss. *J Bone Miner Res.* 2003;18:2152–2158.
- Young MF, Bi Y, Ameye L, Chen XD. Biglycan knockout mice: new models for musculoskeletal diseases. *Glycoconj J.* 2002;19:257–262.
- Corsi A, Xu T, Chen XD, Boyde A, Liang J, Mankani M, Sommer B, Iozzo RV, Eichstetter I, Robey PG, Bianco P, Young MF. Phenotypic effects of biglycan deficiency are linked to collagen fibril abnormalities, are synergized by decorin deficiency, and mimic Ehlers-Danlos-like changes in bone and other connective tissues. *J Bone Miner Res.* 2002;17:1180–1189.
- Amye L, Aria D, Jepsen K, Oldberg A, Xu T, Young MF. Abnormal collagen fibrils in tendons of biglycan/fibromodulin-deficient mice lead to gait impairment, ectopic ossification, and osteoarthritis. *FASEB J.* 2002;16:673–680.
- Yeo TK, Torok MA, Kraus HL, Evans SA, Zhou Y, Marcum JA. Distribution of biglycan and its propeptide form in rat and bovine aortic tissue. *J Vasc Res.* 1995;32:175–182.
- Gutierrez PS, Reis MM, Higuchi ML, Aiello VD, Stolf NA, Lopes EA. Distribution of hyaluronan and dermatan/chondroitin sulfate proteoglycans in human aortic dissection. *Connect Tissue Res.* 1998;37:151–161.
- Melrose J, Whitlock J, Xu Q, Ghosh P. Pathogenesis of abdominal aortic aneurysms: possible role of differential production of proteoglycans by smooth muscle cells. *J Vasc Surg.* 1998;28:676–686.
- Tamarina NA, Grassi MA, Johnson DA, Pearce WH. Proteoglycan gene expression is decreased in abdominal aortic aneurysms. *J Surg Res.* 1998;74:76–80.
- Armstrong PJ, Johanning JM, Calton WC Jr, Delatore JR, Franklin DP, Han DC, Carey DJ, Elmore JR. Differential gene expression in human abdominal aorta: aneurysmal versus occlusive disease. *J Vasc Surg.* 2002;35:346–355.
- Theocharis AD, Karamanos NK. Decreased biglycan expression and differential decorin localization in human abdominal aortic aneurysms. *Atherosclerosis.* 2002;165:221–230.
- Dmowski AT, Carey MJ. Aortic dissection. *Am J Emerg Med.* 1999;17:372–375.
- Nienaber CA, Eagle KA. Aortic dissection: new frontiers in diagnosis and management: part I: from etiology to diagnostic strategies. *Circulation.* 2003;108:628–635.
- Hasham SN, Lewin MR, Tran VT, Pannu H, Muilenburg A, Willing M, Milewicz DM. Nonsyndromic genetic predisposition to aortic dissection: a newly recognized, diagnosable, and preventable occurrence in families. *Ann Emerg Med.* 2004;43:79–82.

18. Pannu H, Fadulu VT, Chang J, Lafont A, Hasham SN, Sparks E, Giampietro PF, Zaleski C, Estrera AL, Safi HJ, Shete S, Willing MC, Raman CS, Milewicz DM. Mutations in transforming growth factor-beta receptor type II cause familial thoracic aortic aneurysms and dissections. *Circulation*. 2005;112:513–520.
19. Hasham SN, Willing MC, Guo D, Muilenburg A, He R, Tran VT, Scherer SE, Shete SS, Milewicz DM. Mapping a locus for familial thoracic aortic aneurysms and dissections (TAAD2) to 3p24–25. *Circulation*. 2003;107:3184–3190.
20. Zhu L, Vranckx R, Khau Van Kien P, Lalande A, Boisset N, Mathieu F, Wegman M, Glancy L, Gasc JM, Brunotte F, Bruneval P, Wolf JE, Michel JB, Jeunemaitre X. Mutations in myosin heavy chain 11 cause a syndrome associating thoracic aortic aneurysm/aortic dissection and patent ductus arteriosus. *Nature Genet*. 2006;38:343–349.
21. Guo D, Hasham S, Kuang S-Q, Vaughan CJ, Boerwinkle E, Chen H, Abuelo D, Dietz HC, Basson CT, Shete SS, Milewicz DM. Familial thoracic aortic aneurysms and dissections: genetic heterogeneity with a major locus mapping to 5q13–14. *Circulation*. 2001;103:2461–2468.
22. Kakko S, Raisanen T, Tamminen M, Airaksinen J, Groundstroem K, Juvonen T, Ylitalo A, Uusimaa P, Savolainen MJ. Candidate locus analysis of familial ascending aortic aneurysms and dissections confirms the linkage to the chromosome 5q13–14 in Finnish families. *J Thorac Cardiovasc Surg*. 2003;126:106–113.
23. Coady MA, Davies RR, Roberts M, Goldstein LJ, Rogalski MJ, Rizzo JA, Hammond GL, Kopf GS, Eleftheriades JA. Familial patterns of thoracic aortic aneurysms. *Arch Surg*. 1999;134:361–367.
24. Lin AE, Lippe BM, Geffner ME, Gomes A, Lois JF, Barton CW, Rosenthal A, Friedman WF. Aortic dilation, dissection, and rupture in patients with Turner syndrome. *J Pediatr*. 1986;109:820–826.
25. Proctor GB, Horobin RW. Chemical structures and staining mechanisms of Weigert's resorcin-fuchsin and related elastic fiber stains. *Stain Technol*. 1988;63:101–111.
26. Fisher LW, Stubbs JT 3rd, Young MF. Antisera and cDNA probes to human and certain animal model bone matrix noncollagenous proteins. *Acta Orthop Scand Suppl*. 1995;266:61–65.
27. Wagner RC. The effect of tannic acid on electron images of capillary endothelial cell membranes. *J Ultrastruct Res*. 1976;57:132–139.
28. Danielson KG, Baribault H, Holmes DF, Graham H, Kadler KE, Iozzo RV. Targeted disruption of decorin leads to abnormal collagen fibril morphology and skin fragility. *J Cell Biol*. 1997;136:729–743.
29. Liu X, Wu H, Byrne M, Krane S, Jaenisch R. Type III collagen is crucial for collagen I fibrillogenesis and for normal cardiovascular development. *Proc Natl Acad Sci U S A*. 1997;94:1852–1856.
30. Bianco P, Riminucci M, Silvestrini G, Bonucci E, Termine JD, Fisher LW, Robey PG. Localization of bone sialoprotein (BSP) to Golgi and post-Golgi secretory structures in osteoblasts and to discrete sites in early bone matrix. *J Histochem Cytochem*. 1993;41:193–203.
31. Pannese E, Procacci P. Ultrastructural localization of NGF receptors in satellite cells of the rat spinal ganglia. *J Neurocytol*. 2002;31:755–763.
32. Danielsen CC, Andreassen TT. Mechanical properties of rat tail tendon in relation to proximal-distal sampling position and age. *J Biomech*. 1988;21:207–212.
33. Saruk M, Eisenstein R. Aortic lesion in Marfan syndrome: the ultrastructure of cystic medial degeneration. *Arch Pathol Lab Med*. 1977;101:74–77.
34. Marsalese DL, Moodie DS, Lytle BW, Cosgrove DM, Ratliff NB, Goormastic M, Kovacs A. Cystic medial necrosis of the aorta in patients without Marfan's syndrome: surgical outcome and long-term follow-up. *J Am Coll Cardiol*. 1990;16:68–73.
35. Baccarani-Conti M, Vincenzi D, Cicchetti F, Mori G, Pasquali-Ronchetti I. Immunocytochemical localization of proteoglycans within normal elastin fibers. *Eur J Cell Biol*. 1990;53:305–312.
36. Holbrook KA, Byers PH. Structural abnormalities in the dermal collagen and elastic matrix from the skin of patients with inherited connective tissue disorders. *J Invest Dermatol*. 1982;79(suppl 1):7s–16s.
37. Hausser I, Anton-Lamprecht I. Differential ultrastructural aberrations of collagen fibrils in Ehlers-Danlos syndrome types I-IV as a means of diagnostics and classification. *Hum Genet*. 1994;93:394–407.
38. Tzaphlidou M. Diameter distributions of collagenous tissues in relation to sex. A quantitative ultrastructural study. *Micron*. 2001;32:333–336.
39. Maki JM, Rasanen J, Tikkanen H, Sormunen R, Makikallio K, Kivirikko KI, Soininen R. Inactivation of the lysyl oxidase gene *Lox* leads to aortic aneurysms, cardiovascular dysfunction, and perinatal death in mice. *Circulation*. 2002;106:2503–2509.
40. Reinboth B, Hanssen E, Cleary EG, Gibson MA. Molecular interactions of biglycan and decorin with elastic fiber components: biglycan forms a ternary complex with tropoelastin and microfibril-associated glycoprotein 1. *J Biol Chem*. 2002;277:3950–3957.
41. Trask TM, Trask BC, Ritty TM, Abrams WR, Rosenbloom J, Mecham RP. Interaction of tropoelastin with the amino-terminal domains of fibrillin-1 and fibrillin-2 suggests a role for the fibrillins in elastic fiber assembly. *J Biol Chem*. 2000;275:24400–24406.
42. Amey L, Young MF. Mice deficient in small leucine-rich proteoglycans: novel in vivo models for osteoporosis, osteoarthritis, Ehlers-Danlos syndrome, muscular dystrophy, and corneal diseases. *Glycobiology*. 2002;12:107R–116R.
43. Trask BC, Trask TM, Broekelmann T, Mecham RP. The microfibrillar proteins MAGP-1 and fibrillin-1 form a ternary complex with the chondroitin sulfate proteoglycan decorin. *Mol Biol Cell*. 2000;11:1499–1507.
44. Hayward CS, Kelly RP, Collins P. The roles of gender, the menopause and hormone replacement on cardiovascular function. *Cardiovasc Res*. 2000;46:28–49.
45. Ailawadi G, Eliason JL, Roelofs KJ, Sinha I, Hannawa KK, Kaldjian EP, Lu G, Henke PK, Stanley JC, Weiss SJ, Thompson RW, Upchurch GR Jr. Gender differences in experimental aortic aneurysm formation. *Arterioscler Thromb Vasc Biol*. 2004;24:2116–2122.
46. Park KM, Kim JJ, Ahn Y, Bonventre AJ, Bonventre JV. Testosterone is responsible for enhanced susceptibility of males to ischemic renal injury. *J Biol Chem*. 2004;279:52282–52292.
47. Vamvakopoulos NC, Chrousos GP. Evidence of direct estrogenic regulation of human corticotropin-releasing hormone gene expression: potential implications for the sexual dimorphism of the stress response and immune/inflammatory reaction. *J Clin Invest*. 1993;92:1896–1902.

CLINICAL PERSPECTIVE

For the majority of cases of spontaneous aortic dissection and rupture in humans, the cause is unknown. An inherited risk is associated with genetic syndromes and with loci mapped to diverse autosomal chromosomes. Analysis of pedigrees has indicated that the risk for aortic dissection may also be inherited as an X-linked trait. The biglycan gene, found on chromosome X in humans and mice, encodes a small leucine-rich proteoglycan involved in the integrity of the extracellular matrix. Abnormalities in biglycan expression have been described in diverse vascular disease, such as aortic aneurysm and dissection. Although primary genetic defects in the biglycan gene have not been reported in humans, biglycan mRNA and protein expression is reduced in patients with Turner syndrome, in which aortic dissection and rupture are common. We observed aortic dissection and rupture in male biglycan knockout mice. The aortas showed structural abnormalities of collagen fibrils and reduced tensile strength. Similar collagen fibril changes were observed in both male and female biglycan-deficient mice, a finding that implies additional determinants such as gender-related response to stress in the development of this vascular catastrophe only in male mice. This study points to the biglycan gene as a candidate gene for the risk of aortic dissection and rupture in humans. If confirmed, this could be useful for identifying patients at risk in the future.